Earth's Future

RESEARCH ARTICLE

10.1029/2021EF002461

Key Points:

- Deposited sediment volumes in the Yangtze River Delta (YRD) are calculated for 500-year intervals over the last 2000 years for the first time
- Sediment accumulation rate in the last 0.5 ka doubles that of the warmer 1.0–0.5 ka period
- Human activities are the main driver of the accelerated growth of the YRD over the last 500 years

Supporting Information:

Supporting Information may be found in the online version of this article.

Correspondence to:

W. Zhang,
wgzhang@sklec.ecnu.edu.cn

Citation:

Nian, X., Zhang, W., Wang, X., Hutchinson, S. M., Zhao, X., & Liu, K.-b. (2022). Multi-centennial variability of Yangtze delta growth over the last 2000 years: Interplay of climate and people. *Earth's Future*, *10*, e2021EF002461. https://doi.org/10.1029/2021EF002461

Received 29 SEP 2021
Accepted 11 JUL 2022

Multi-Centennial Variability of Yangtze Delta Growth Over the Last 2000 Years: Interplay of Climate and People

Xiaomei Nian[1], Weiguo Zhang[1], Xiaoting Wang[1], Simon M. Hutchinson[2], Xuanqi Zhao[1], and Kam-biu Liu[3]

[1]State Key Laboratory of Estuarine and Coastal Research, East China Normal University, Shanghai, China, [2]School of Science, Engineering and Environment, University of Salford, Greater Manchester, UK, [3]Department of Oceanography and Coastal Sciences, Louisiana State University, Baton Rouge, LA, USA

Abstract Reconstruction of sediment accumulation in river deltas over the Holocene provides a basis for understanding the relationship between climate change, human activities and delta growth. However, variations in deposition rates on a centennial-scale over the last 2000 years remain poorly studied for mega-deltas. Based on optically stimulated luminescence and AMS ^{14}C ages, we calculated deposited sediment volumes in the Yangtze River Delta (YRD) for 500-year intervals over the last two millennia for the first time. Our results reveal that the 2.0–1.5 and 0.5–0 ka periods had higher sediment deposition rates than in 1.5–1.0 and 1.0–0.5 ka, with maximum value about two times that of the minimum. A comparison with historical records of flooding and drought events indicates that a wetter climate led to a higher sediment deposition, reflecting the role of fluvial discharge in delta growth. However, the highest sediment deposition ($205 \pm 29 \times 10^6$ m^3/a) over the last 500 years is not only related to the wetter conditions of the Little Ice Age, but also linked to dramatic regional population growth. We suggest that human activities have predominated over natural forcing in determining the deltaic growth over the last five centuries. Taking the Medieval Climate Anomaly with the lowest deposition volume as an analog of current climate warming, and considering the decline in sediment loads due to recent damming and soil conservation, the YRD is likely to face an even more severe deficit in sediment supply and higher risk of delta destruction in the coming centuries.

Plain Language Summary Delta growth is influenced by both climate change and human activities through the production of sediments in the catchment, their transportation toward the coast, and storage in the delta region. Research on centennial-scale delta evolution over the last 2000 years is critical for understanding delta development mechanisms and future trends. However, this information is relatively scarce, as delta deposits are difficult to date. In this paper, based on a combination of newly obtained optically stimulated luminescence ages and existing records, sediment deposition volumes were calculated for 500-year intervals over the last 2000 years. The results show that deposition volumes peaked over the most recent 500 years spanning the wetter climatic conditions of the Little Ice Age. In addition to the role played by climate in the centennial fluctuations in depositional volume, human activity has led to a dramatic increase of delta growth rate over the last five centuries. Using the warmer 1.0–0.5 ka period with the lowest sediment accumulation rate as an analogue to future climate warming, we suggest that the Yangtze River Delta will experience a much reduced growth rate and therefore a greater impact on this densely populated region from sea level rise in the coming centuries.

1. Introduction

Globally, river deltas are home to more than 500 million people (Ericson et al., 2006; Syvitski et al., 2009). The formation of deltas is influenced by both climate characteristics and human activities, which determine sediment production, transport, storage, and deposition on its pathway from the drainage basin to the coast (Allen, 2017). In the present context of declining fluvial sediment loads and sea-level rise, deltas face an increased risk of erosion, which seriously threatens human occupation and sustainable development in deltaic regions (Syvitski et al., 2009). Considering that modern river deltas are the product of an evolution over ca. 8000 years (Stanley & Warne, 1994), there is an urgent need to understand delta evolution mechanisms at various timescales to prepare for future challenges. Hence, a number of studies have been carried out to reconstruct the trajectories of delta growth in the past (de Haas et al., 2018; Hobo et al., 2014; Li et al., 2003; Middelkoop et al., 2010; Wang et al., 2018). Through high-resolution stratigraphic and chronological analysis, reconstruction of sediment depositional volumes can provide a better understanding of delta development and its response to climate change and human activities (de Haas et al., 2018).

Although millennial-scale variations in coastline migration and accumulated sediment volume have been reported for several deltas (Nageswara Rao et al., 2015; Tamura et al., 2009; Wang et al., 2018), centennial scale delta evolution over the last 2000 years, a period of marked climate changes as well as increasing human activity, remains poorly studied (Maselli & Trincardi, 2013), especially for large river deltas in Asia. This paucity partly reflects the poor chronological constraint on deltaic deposits using ^{14}C as a dating technique. This is caused by the scarcity of dateable carbon material in sandy mouth bar deposits and/or the delayed input of aged carbon from the catchment. In Holocene deltaic sediments, it has been found that samples usually yield ^{14}C dates that are too old and commonly inverted in stratigraphy due to the storage and reworking of older deposits in the catchment and delta environments (Stanley & Chen, 2000). However, the development of optically stimulated luminescence (OSL) dating (Huntley et al., 1985) provides a solution to these limitations (e.g., Chamberlain et al., 2018; Nian & Zhang, 2018; Shen et al., 2015; Tamura et al., 2012). Furthermore, the relative importance of human activities versus climate change in delta evolution remains an issue of debate (Ibáñez et al., 2019; Maselli & Trincardi, 2013). Based on studies on deltas in the Mediterranean and the Black Sea, Maselli and Trincardi (2013) suggested that human activities have dominated delta growth over the last 2000 years. However, Ibáñez et al. (2019) suggested that both climate and physical setting in the marine environment play dominant roles (e.g., fluvial discharge and continental shelf slope) according to a statistical analysis of a global data set of observations spanning 86 deltas.

The Yangtze River Delta (YRD) is a delta that experiences strong fluvial-tidal interaction, which is also evident in a number of river deltas, particularly densely populated mega deltas in Asia. It also hosts the most active economic center in China. Studies on modern delta processes and millennial scale evolution have received great attention (e.g., Chen et al., 1988; Li et al., 2000; Wang et al., 2018). In terms of centennial variability in delta growth, studies using historical documents and geomorphological surveys have provided a framework for coastline shifts within the last 2000 years (e.g., Chen et al., 1979; Zhang, 1998). However, three-dimensional stratigraphic analysis lacks a solid chronological control. In this study, based on a synthesis of 245 dates from 42 cores, delta growth and the volume of deposits over the YRD during the last 2000 years have been reconstructed in 500-year interval for the first time. By comparing with available proxies of climate change (i.e., flood/drought occurrence (Zheng et al., 2014), river water level (Qin et al., 2020) and temperature (Ge et al., 2003)) and human activities (i.e., population (National Bureau of Statistics of China, 1953–2010; Zhang, 2000)), we elucidate the relative influence of climate and anthropogenic forcing on delta growth at multi-centennial timescale to offer a perspective on future delta evolution under a warming climate.

2. Study Area and Methods

2.1. The Yangtze River Delta

The Yangtze River originates on the Tibet Plateau and flows from west to east along a course of ~6,300 km. It has a large drainage basin with a very dense population (presently ~500 million people over an area of 1.8 million km^2) concentrated in the middle to lower reaches of the catchment. Rainfall and fluvial discharge in the Yangtze River's catchment are influenced by the East Asian Summer Monsoon (EASM), although in southwestern China, that is, the upper reaches of the river, the climate is controlled by the Indian summer monsoon (ISM) (Zhang et al., 2019) (Figure 1a). The monsoon climate displays significant variabilities in rainfall at millennial, centennial, decadal and seasonal timescales (e.g., Wang et al., 2005). As a reflection of rainfall and fluvial discharge variability, sediment load also shows marked variations, as evident in both modern observations and reconstructed sediment depositional volumes in the delta (e.g., Wang et al., 2018; Yang et al., 2015).

The evolution of the delta during the Holocene has resulted in a huge subaerial (~30,000 km^2) and subaqueous (~10,000 km^2) delta (Li et al., 2011). The YRD has prograded rapidly over the last two millennia in response to an increased supply of sediment from upstream due to intensified human activities (Chen et al., 1979; Li et al., 2000). Previous studies have shown that the YRD was a funnel shaped estuary 2000 years ago with the apex located between Zhenjiang and Yangzhou (Chen et al., 1979) (Figure 1b). Stratigraphic studies have revealed that the deposits over the last 2000 years reach a thickness of ~20 m in the paleo-incised valley in the northern part of the delta, which becomes shallower toward its southern flank (e.g., Hori et al., 2001; Wang et al., 2019). The

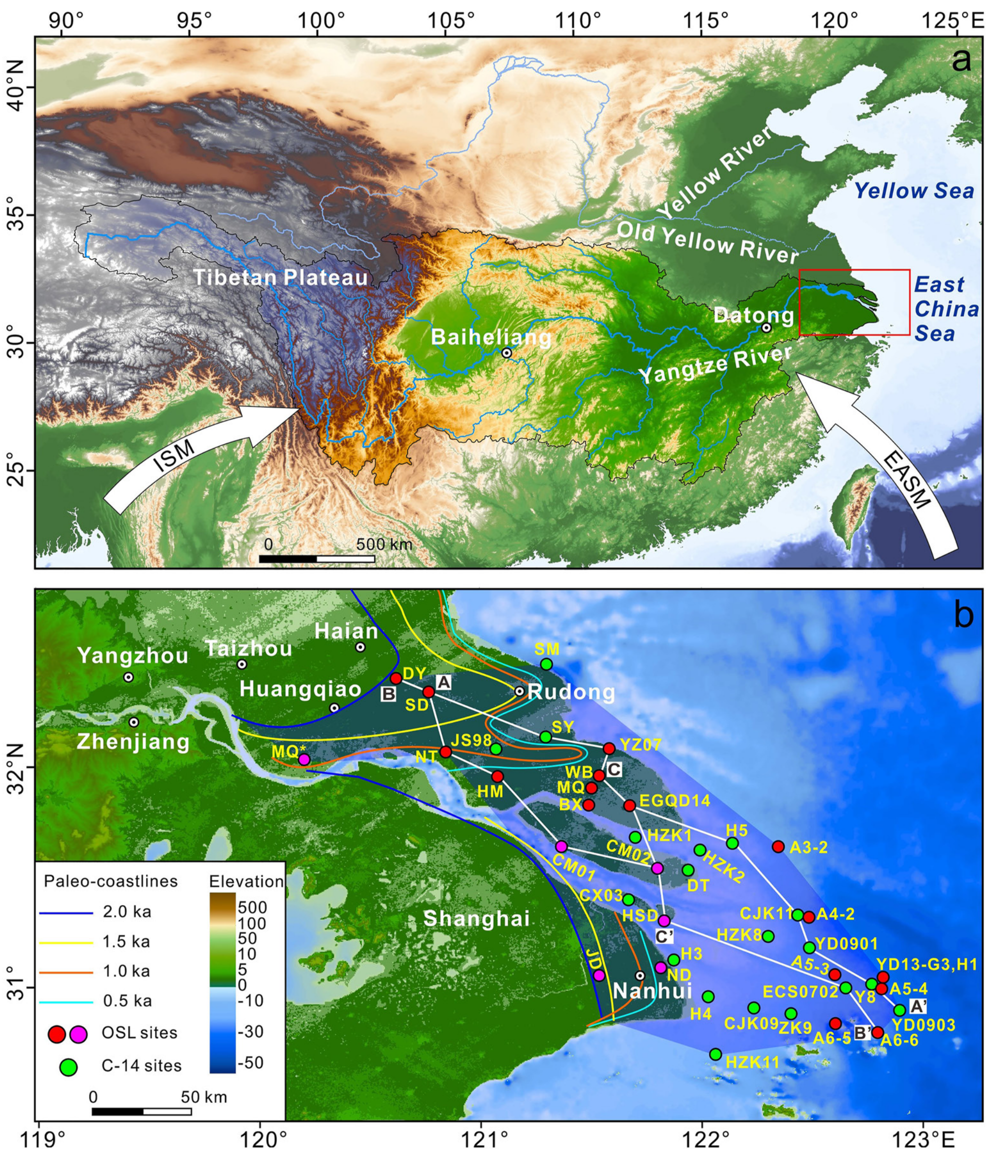

Figure 1. Location of the Yangtze River basin (a), and the red square depicts the location of the Yangtze River Delta (YRD) which is detailed in (b). a, The trajectories of the East Asian summer monsoon and Indian summer monsoon are shown by the white arrows. The white circles are historic water level markers on the Yangtze River at Baiheliang (Qin et al., 2020) and Datong Hydrological Station which gauges fluvial sediment flux to the sea. b, The red/magenta and green circles represent the cores dated by the optically stimulated luminescence and AMS ^{14}C techniques, respectively. Red circles represent published cores while magenta new dated cores. Detailed core information can be found in Table S1 in Supporting Information S1, Table S2 and Table S3. Cores along three transects (white lines, A-A', B-B', C-C') are used to construct the stratigraphy shown in Figure 2. The paleo-coastlines of the YRD over the last 2 ka follow previous studies (Chen et al., 1979; Delta Research Group, 1978) with modification according to the compilation of recent dating results. The blue-shaded zone indicates the area for which sediment deposition volume has been calculated.

deposits change from silty shallow marine/prodelta facies, sandy delta front platform (e.g., mouth bar) facies, to silty delta plain faces in ascending order (Wang et al., 2019). With delta progradation, the upper mouth bar and delta plain facies have migrated east- and south-ward (Figure 1b; Chen et al., 1979).

2.2. Chronology, Sediment Accumulation Volume and Land Area Calculation

We have conducted luminescence dating on 17 Holocene sediment cores in the YRD and some of these data have been published (Table S2). In this study, OSL dating was further carried out on 52 samples from six cores

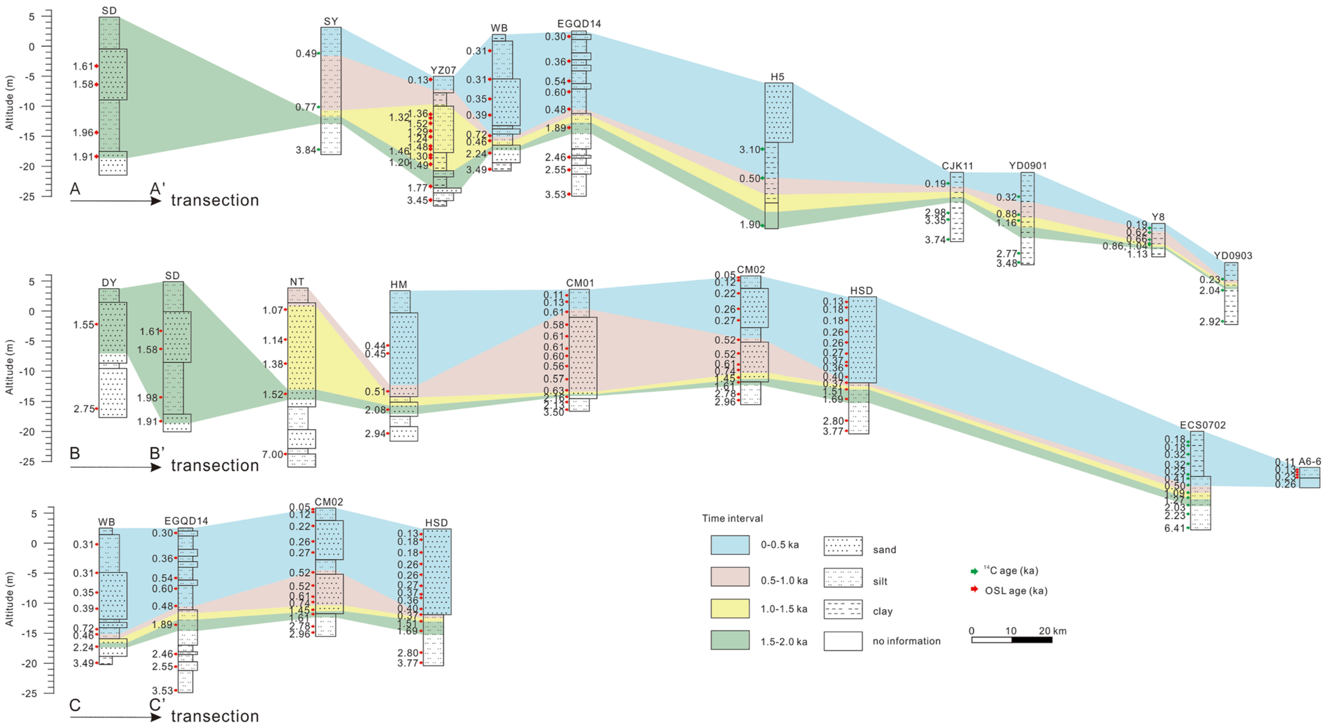

Figure 2. Stratigraphy along two longitudinal (A-A', B-B') and one transverse (C-C') sections with 500-year intervals shown in different colors. Detailed age and isochron information are presented in Tables S1 and S4 in Supporting Information S1, Table S2 and Table S3. All the OSL and ^{14}C ages were converted to ka relative to 2020 CE.

(Table S1 in Supporting Information S1), which were collected from Chongming Island (core CM01, CM02), Hengsha Island (core HSD), Maqiao (MQ), Jiandong (JD), and Niudu (ND) in the YRD (Figure 1b). The drilling was performed using a rotary-pressure mechanism method with a total core recovery value greater than 90%. Additional information about these six cores is available in Text S1 and Figure S1 in Supporting Information S1. Detailed descriptions of OSL sample pretreatment and measurement are presented in Text S2 in Supporting Information S1.

In the study area, all the previously published sediment cores with reliable age controls were included (Figure 1b). These relatively evenly distributed cores can reflect the three-dimensional stratigraphic structure over the study area in general (as shown in Figure 2). Through the integration of new data (52 ages from 6 cores, magenta circles in Figure 1b, Table S1 in Supporting Information S1) and 193 previously published ages, including 114 OSL samples (17 cores, red circles in Figures 1b and Tables S2) and 79 AMS ^{14}C samples (19 cores, green circles in Figures 1b and Table S3), centennial-scale sediment accumulation volume and land area were calculated for 500-year intervals spanning the last 2000 years. As shown in previous studies, AMS ^{14}C ages often yield older or reversed ages due to the complex transport and deposition of exogenous carbon from the catchment to delta (Stanley & Chen, 2000). This is further confirmed by our studies (Nian et al., 2021; Nian & Zhang, 2018). Therefore, this paper uses only the OSL ages for these cores dated by two methods. Isochrons at 2, 1.5, 1 and 0.5 ka were determined by linear interpolation of the ages obtained for the late Holocene sediments of the YRD (Table S4 in Supporting Information S1). From these data, the volume of deposited sediment were calculated using ArcGIS 10.5. In ArcGIS, the triangulated irregular network (TIN) tool was used to create TINs for the surface elevations and elevations of control points at each age (0.5, 1, 1.5 and 2 ka) of the cores. Then we used the TIN to Raster tool to convert the above TINs into the corresponding raster data, and finally the Cut Fill tool from ArcGIS Spatial Analyst was used as well to calculate the volume of sediments in each 500-year interval. Land areas were calculated according to the paleo-coastlines of the YRD over the last 2 ka (Figure 1a).

According to the stratigraphic reconstruction (Figure 2), we find that isochronic layers between the cores with longer distance (e.g., HSD and ECS0702) parallel each other, implying relatively homogeneous accretion along the progradation direction. Therefore, we assume linear change between neighboring cores when carrying

Table 1
Deposited Sediment Volume and Land Area Growth Over the Last 2000 Years

Time period (ka)	Total volume of trapped sediment (10^9 m^3)	Accumulation rate by volume (10^6 m^3/a)	Land area growth (km^2)
2.0–0	304 ± 43	152 ± 21	10,803 ± 108
2.0–1.5	80 ± 11	161 ± 23	2298 ± 230
1.5–1.0	63 ± 9	125 ± 18	2742 ± 274
1.0–0.5	59 ± 8	118 ± 17	1638 ± 164
0.5–0	102 ± 14	205 ± 29	4125 ± 413

out interpolation. Hence, in the calculation of accumulation volume, we consider only the error of ascribing depth of isochronic layers. The depths of these controlling points for each core are obtained by age-depth model of linear interpolation between adjacent dated points. Since typical total estimated uncertainties are 5%–10% for the OSL age (Murray et al., 2021) and less than 2% for the AMS ^{14}C age (Guilderson et al., 2005), we assumed that the depth error is 10%. Similarly, the estimation of uncertainty in land areas is also assumed to be 10%. Finally, an approximate uncertainty of 14% was introduced into the volume calculations for different time periods according to the method of error propagation (Table 1).

3. Results

3.1. Spatial Growth of Delta

The stratigraphic cross-sections A-A', B-B' and C-C' (Figure 2) show upper sandy mouth bar facies overlying silty/clayey prodelta facies in cores sampled onshore and from the islands of the estuary. In the present subaqueous delta, such stratigraphic architecture is replaced by homogeneous delta front slope/prodelta facies with increasing water depth. Dating results reveal a deltaic progradation trend from northwest to southeast. Since cores DY, SD and NT are located in a nearly north-south orientation, the spatial distribution of their stratigraphy reflects a southward progradation during the 2.0–1.5 ka period, with the delta front toe located around a line connecting cores SY and NT. Between 1.5 and 1.0 ka, the delta front/prodelta transition had only been pushed to the site of core HM. Between 1.0 and 0.5 ka, the mouth bar shifted to the western part of Chongming Island (e.g., core CM01) and the delta front/prodelta transition was located on a line connecting cores HSD and H5. Over the last 0.5 ka, the sites of cores CM02, HSD and H5 became mouth bars and the delta front slope prograded to the site of core A6-6 at a current water depth of 26 m. Clearly, coastline change shows large variability, with the smallest progradation occurring in the 1.0–0.5 ka period (Figure 1). According to reconstructed stratigraphy, the delta front slope is steeper for the period 2–1 ka than that of 1–0 ka, with the last 0.5 ka exhibiting the greatest extension of delta front deposit (Figure 2).

3.2. Variability of Sediment Accumulation Volume and Land Area Growth

Marked multi-centennial variability exists in the sediment accumulation rate during the last 2 ka. The volume of deposited sediment during the past 2 ka averaged 152 × 10^6 m^3/a (Table 1), which approximately equals the previously reported value for this period of 129 × 10^6 m^3/a (Wang et al., 2018). The highest accumulation rate is observed over the last 500 years, which is also the highest over the Holocene (Figure 3). Based on bathymetric chart comparison, Shen et al. (1983) calculated a deposition rate of 160 × 10^6 m^3/a between 1958 and 1978 in the delta, which is also lower than that of the last 0.5 ka. This highest value is followed by the period 2.0–1.5 ka (Table 1). The lowest rate occurred from 1.5 to 0.5 ka, which is approximately one half of the value for the last 0.5 ka. Land area growth was approximately 4.6–5.5 km^2/a at 2.0–1.0 ka, but was found to be drastically decreased to around 3.3 km^2/a at 1.0–0.5 ka (only 60%–71% of 2.0–1.0 ka level) and then increased up to 8.3 km^2/a in the last 0.5 ka (Table 1).

4. Discussion and Conclusions

4.1. Delta Growth: Area Versus Volume

Many studies have used subaerial delta area to indicate delta growth (e.g., Ibáñez et al., 2019), as this variable can be easily determined. In fact, sediments deposited in the delta are partitioned into subaerial and subaqueous parts, and land growth is determined by both aggradation and progradation of the subaqueous delta (Shen et al., 1983). The periods of 1.5–1.0 ka and 1.0–0.5 ka have similar accumulated sediment volumes, yet the former shows a larger subaerial delta growth than the latter (Table 1, Figure 1). The stratigraphic evidence indicates that the former period witnesses much steeper delta front deposit than the later (Figure 2). It is interesting to note that the aggradation of subaqueous delta for the 1.0–0.5 ka occurred mainly in the period 0.8–0.5 ka (Figure 2). Historical documents have suggested that coastline progradation occurred until 0.7 ka ago, after which the shoreline

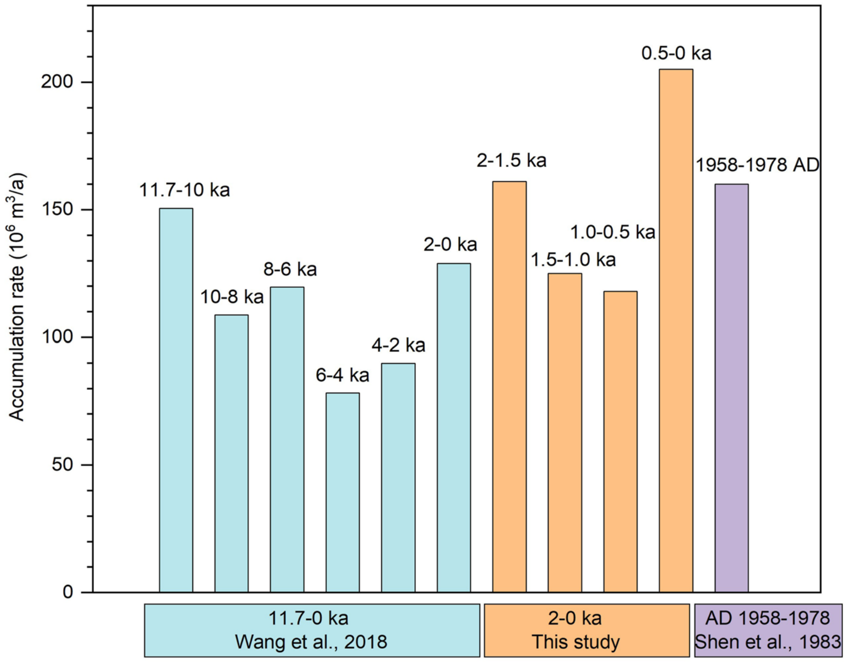

Figure 3. Variations in sediment accumulation rate for the last 2 ka and their comparison with those pre-2 ka (Wang et al., 2018) and 1958–1978 CE (Shen et al., 1983) periods.

retreated until 0.4 ka by a distance of about 35 km (Tan, 1982; Wang et al., 2019). This means that sediment originally comprising subaerial delta was eroded and displaced to the subaqueous delta. Therefore, land area alone is an inadequate reflection of delta growth and maybe misleading without considering the sediment accumulated under water.

4.2. The Relative Importance of Climate and Human Activities

Our investigation reveals that marked multi-centennial variability exists in the sediment accumulation rates of the YRD during the last 2 ka (Table 1, Figure 4a), which can be modulated by climate changes and human activities. Fluvial discharge is an important factor affecting delta growth, as with greater discharge, more fluvial sediment is delivered to the coast (e.g., Ibáñez et al., 2019; Yang et al., 2015). Indices of floods/droughts reconstructed using historical documents can be regarded as proxies of fluvial discharge. They reveal a greater occurrence of extreme flooding events over the periods 2.0–1.5 ka and the last 0.5 ka in the middle-lower Yangtze River region (Figure 4b) (Zheng et al., 2014). Archeological evidence (an inscription on rocks (rockfish)) in the main channel of the upper Yangtze River (Baiheliang, Figure 1) records water level fluctuations during the last 1000 years and indicates that severe droughts occurred more frequently during the warmer Medieval Climate Anomaly (MCA, 950–1250 CE) and relatively less frequently during the cooler Little Ice Age (LIA, 1501–1900 CE) (Figures 4c and 4d) (Qin et al., 2020). Clearly, the change in accumulated sediment volume matches well with the flooding/drought indices, suggesting that higher fluvial discharge leads to greater sediment delivery and sediment deposition in the delta.

However, the last 500 years has a much higher sediment accumulation volume than that of the period of 2.0–1.5 ka, although extreme flooding occurrence is similar for these two periods (Figure 4b). It is well documented that human activities (e.g., land use/land cover change and river engineering) can alter the relationship between fluvial discharge and sediment load (Yang et al., 2015). In the pre-industrial era, deforestation, which has been linked to demand for food and fuel under population growth (Woodbridge et al., 2014), led to greater runoff generation as well as soil erosion (Gentry & Lopez-Parodi, 1980). Enhanced soil erosion can lead to the siltation of river channels and promote flooding, which calls for leveeing for flood control. In a cascade, this can lead to enhanced downstream sediment transport (Figure 5) (Wohl et al., 2015; Yin & Li, 2001).

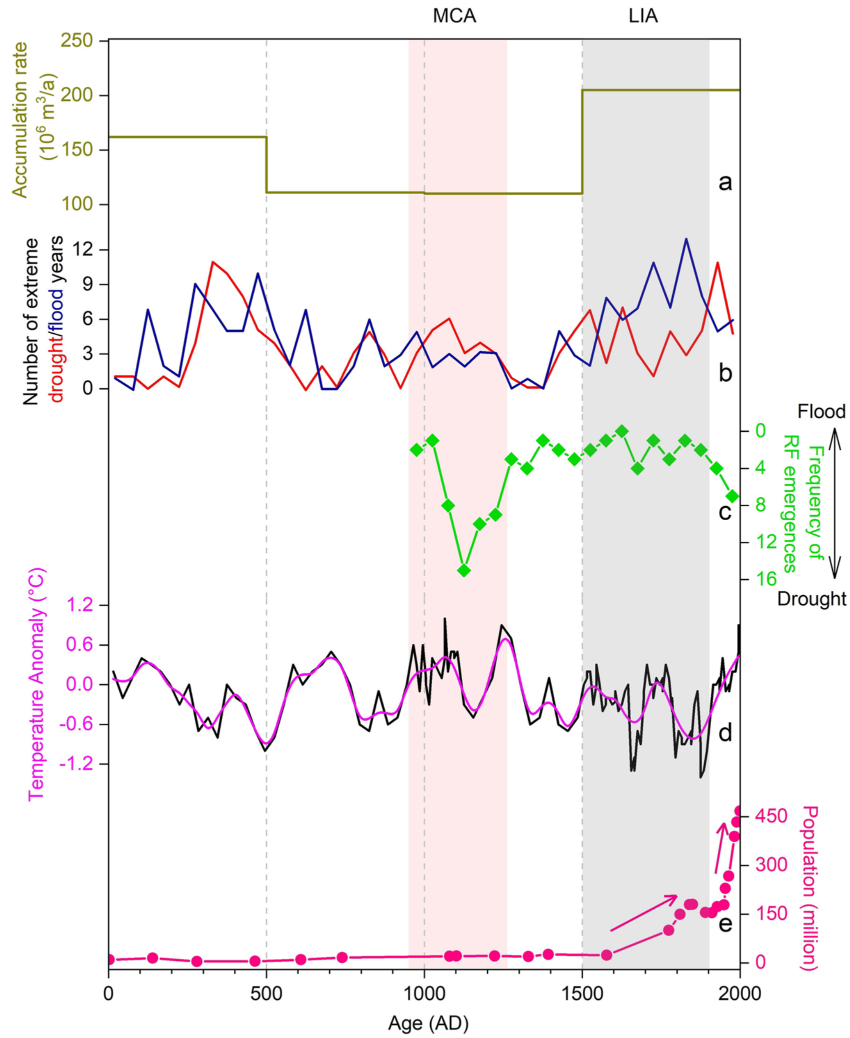

Figure 4. Trends in sediment accumulation rate (a), flood occurrence (b and c), temperature (d), and population variations in the Yangtze River catchment (e) during the last 2000 years a, This study. b, Extreme floods/drought occurrence in 50-year intervals in the Yangtze-Huaihe Region (Zheng et al., 2014). c, Frequency of rockfish emergences in the Yangtze River since 951 CE (Qin et al., 2020). d, Winter half-year temperature anomalies (black line) with a five-point smoothing (magenta line) in East-Central China (Ge et al., 2003). e, Population variations (Data compiled from Zhang (2000) and National Bureau of Statistics of China (1953–2000)). The red and gray bands mark the Medieval Climate Anomaly and Little Ice Age, respectively.

Before the Northern Song Dynasty (960–1127 CE), the population of the Yangtze River's catchment was still relatively low (Figure 4e). Within the last 500 years, however, there has been a dramatic increase in the region's population reflecting the economic growth of southern China due to the southward shifting of the economic center of China since the Southern Song Dynasty (1127–1279 CE) (Han, 2013). The resource demands of population growth promoted the expansion of agriculture across the Yangtze River catchment with deforestation on steeper hillslopes and the mountain regions (Han, 2013). At the same time, the introduction of American crops during the Ming Dynasty (1368–1644 CE) (Ho, 1955), especially sweet potatoes, eased the pressure for food production, but also promoted soil erosion. As a result, local chronicles have recorded the rapid emergence of in-channel bars and floodplain development in the middle reach of the Yangtze Rivers in the Ming and Qing Dynasties (1644–1911 CE), which promoted land reclamation along the rivers and floodplain lakes (Lu, 2016). Sediment crevasse outlets along the Yangtze River and its tributaries were blocked for flood control of such land (Yin & Li, 2001) and consequently, sediments previously deposited as crevasse splay, were less likely to be transferred to the floodplain (Wohl et al., 2015). Hence, sediment loads significantly increased in the river channel and were more likely to be transported downstream into the delta (Figure 5).

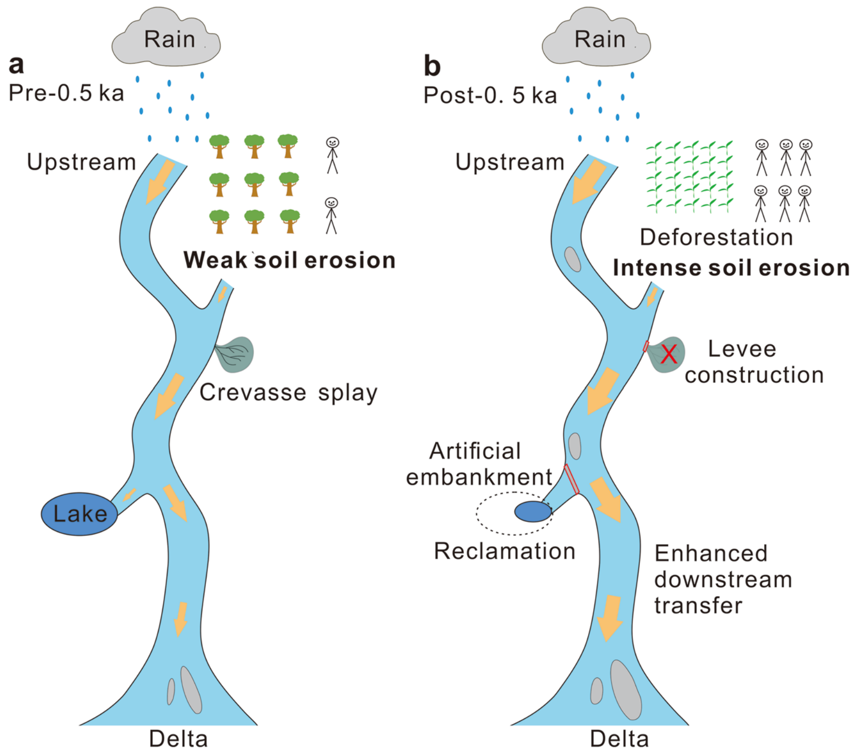

Figure 5. A sketch visualizing the effects of human activities on sediment production and delivery to the delta. (a) Pre-0.5 ka, (b) post-0.5 ka.

The interplay of a greater population, enhanced river channel manipulation, and wetter climate conditions is therefore probably responsible for the dramatic sediment deposition levels in the delta within the last 500 years. It should be noted, however, that, in addition to fluvial sediment from the Yangtze River, sediment discharged into the Yellow Sea via the former course of the Yellow River (1128–1855 CE) and transported by coastal currents southward also contributed to the growth of the YRD over the last millennium, with a pronounced contribution over the last 0.6–0.4 ka (Liu et al., 2010; Shang et al., 2021; Wang et al., 2020; Zhang, 1984). The shift in the course of the Yellow River was also caused by human-caused avulsion due to war at the end of the Northern Song Dynasty (Storozum et al., 2018).

Globally, accelerated delta growth in the last 500 years has been found in deltas in the Mediterranean Sea (Maselli & Trincardi, 2013), the Godavari delta (Nageswara Rao et al., 2015) in the Indian Ocean, and the Mekong delta (Tamura et al., 2020) in the South China Sea. Investigation of the largest southern European deltas showed that delta outbuilding peaked during the LIA in addition to growth during the mild climatic conditions of the Roman Empire (350 BCE–250 CE) (Maselli & Trincardi, 2013). The land area of the Godavari delta in India has averaged 225–301 km^2 during the last 2000–500 years, but increased by 2–3 times (∼632 km^2) over the last 500 years (Nageswara Rao et al., 2015). The muddy deltaic protrusion at Camau within the Mekong delta had an accumulation rate of less than 1 km^2/a before 600 CE, but increased significantly to 4 km^2/a during the last 600 years (Tamura et al., 2020). Although the climatic background is different in these regions (Giosan et al., 2017; Maselli & Trincardi, 2013; Tamura et al., 2020), the increase in population and intensification in agriculture has been proposed as an explanation of the enhanced sediment loads. Our results are consistent with the viewpoint of human dominance over climate drivers in the last 0.5 ka.

4.3. Future Delta Management

The gauged sediment load at Datong Hydrological Station (Figure 1a) in the lower Yangtze River is conventionally used to represent the river's sediment flux. It shows higher values before the 1980s due to intensive deforestation in the river's catchment (average 469 Mt/yr for the period 1958–1978 CE), but declining values toward the present

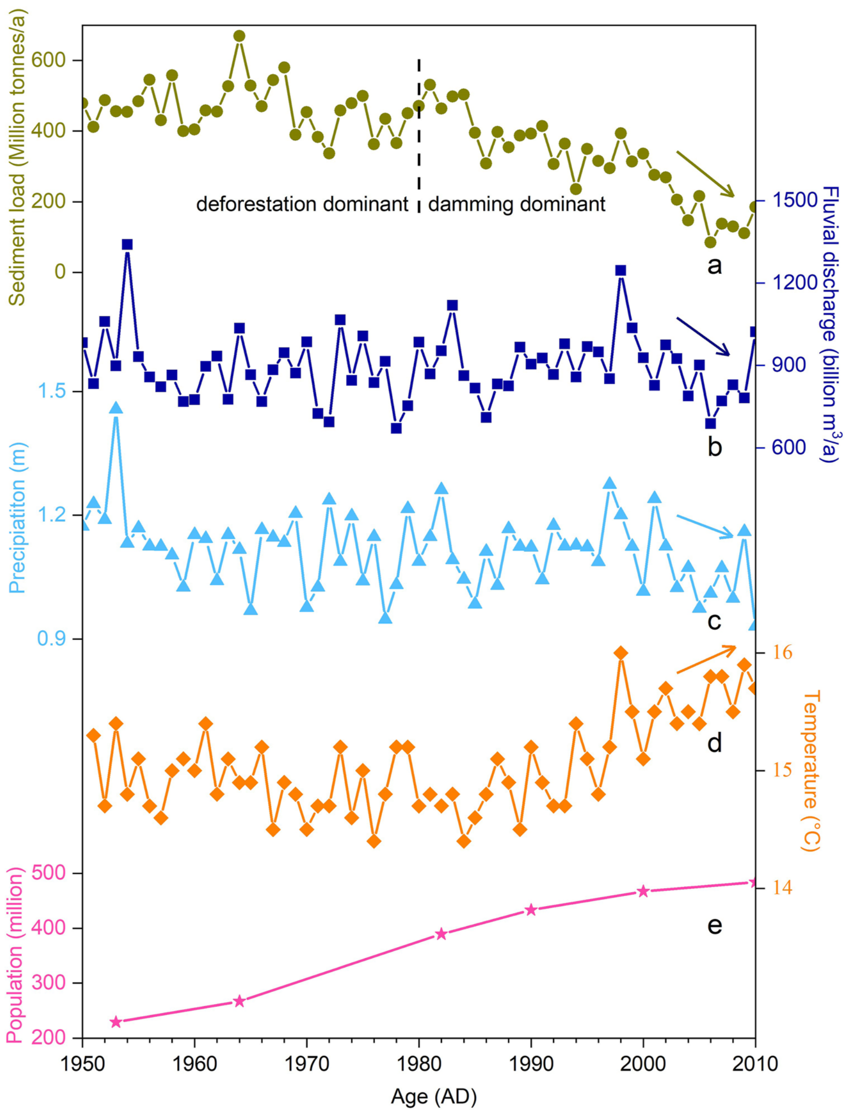

Figure 6. Sediment load and fluvial discharge at Datong Hydrological Station on the Yangtze River (a and b) (Bulletin of Yangtze River Sediment, 1950–2010), precipitation and temperature in the Yangtze River basin (c and d) (Guo et al., 2018) and population change in the Yangtze River basin (e) (National Bureau of Statistics of China, 1953–2010). Arrows highlight recent trends in the curves during 2000–2010.

due to the implementation of soil conservation strategies and tributary damming since the 1980s (Figure 6a) (Yang et al., 2014). The relatively stable fluvial discharge and precipitation over the last 70 years (Figures 6b and 6c) under recent climate warming (Figure 6d) further demonstrates that sediment discharge is strongly influenced by human activities. Significantly, human population growth over the Industrial Era (Figure 6e) has not led to an increased sediment discharge as in the LIA (Figure 4a), which reflects the contrasting impacts of river damming versus catchment deforestation on sediment discharge. In a sense, the recent decline in the fluvial sediment load is reversing the pre-1980s sediment load increase caused by catchment deforestation.

Under the present warming trend, future fluvial discharge in the Yangtze River is still uncertain due to the nonlinearity between fluvial discharge and global climate trends (Zhang et al., 2018). However, geological evidence and historical documents suggest that a warming climate will result in lower rainfall in the Yangtze River basin as the rain belt in East Asia shifts further northward (Zhou et al., 2011). Recent modeling also demonstrates that the fluvial discharge of the Yangtze River will decrease with global warming of less than 1.1°C, but this trend will be reversed beyond a 1.1°C threshold (Zhang et al., 2018). The recent warming trend in the first decade of the 21st century seems to be matched by declining rainfall levels (Figure 6c). If the current warming period has a climate similar to that of MCA, then it is quite likely that sediment deposition volumes will decrease. In combination with further reductions in sediment load due to channel damming and catchment soil conservation, the delta will face an even more severe deficit of sediment supply and higher risk of coastline erosion than anticipated from former studies (e.g., Yang et al., 2014). This study is therefore relevant to environmental management and the challenges of sustainable development in the Yangtze River and other, particularly densely populated, delta locations. Concerns over future delta growth should consider not only recent changes in fluvial sediment load, for example, over the last few decades, but also the longer-term legacy of environmental processes.

Data Availability Statement

The data set is available on the repository Figshare (https://doi.org/10.6084/m9.figshare.14406638).

Acknowledgments
We thank the editor, Amir AghaKouchak, and two anonymous reviewers for their insightful comments and suggestions. Thanks also to Mr. Fengyue Qiu (East China Normal University) for helpful discussions and drawing the figure. We gratefully acknowledge the financial support for this study provided by the National Key Research and Development Program of China (2017YFE0107400), National Natural Science Foundation of China (41771009; 42171009; 41271223), China Postdoctoral Special Science Foundation (2017T100284), China Postdoctoral Science Foundation (2015M571521) and the Open Research Fund of the State Key Laboratory of Estuarine and Coastal Research (SKLEC-PGKF201906).

References

Allen, P. A. (2017). *Sediment routing systems: The fate of sediment from source to sink*. Cambridge University Press.

Bulletin of Yangtze River Sediment. (1950–2010). (In Chinese), Retrieved from http://www.cjw.gov.cn

Chamberlain, E. L., Törnqvist, T. E., Shen, Z., Mauz, B., & Wallinga, J. (2018). Anatomy of Mississippi Delta growth and its implications for coastal restoration. *Science Advances*, *4*(4), eaar4740. https://doi.org/10.1126/sciadv.aar4740

Chen, J., Shen, H., & Yun, C. (1988). *Processes of dynamics and geomorphology of the Yangtze estuary*. (In Chinese). Shanghai Scientific and Technical Publishers.

Chen, J., Yun, C., Xu, H., & Dong, Y. (1979). The developmental model of the Chang Jiang River estuary during last 2000 years. (In Chinese). *Acta Oceanologica Sinica*, *1*, 103–111.

de Haas, T., Pierik, H. J., van der Spek, A. J. F., Cohen, K. M., van Maanen, B., & Kleinhans, M. G. (2018). Holocene evolution of tidal systems in The Netherlands: Effects of rivers, coastal boundary conditions, eco-engineering species, inherited relief and human interference. *Earth-Science Reviews*, *177*, 139–163. https://doi.org/10.1016/j.earscirev.2017.10.006

Delta Research Group, Department of Marine Geology, Tongji University. (1978). Holocene formation and development of the Yangtze delta. *Chinese Science Bulletin*, *35*, 310–313. (In Chinese).

Ericson, J. P., Vörösmarty, C. J., Dingman, S. L., Ward, L. G., & Meybeck, M. (2006). Effective sea-level rise and deltas: Causes of change and human dimension implications. *Global and Planetary Change*, *50*(1), 63–82. https://doi.org/10.1016/j.gloplacha.2005.07.004

Ge, Q., Zheng, J., Fang, X., Man, Z., Zhang, X., Zhang, P., & Wang, W. C. (2003). Winter half-year temperature reconstruction for the middle and lower reaches of the Yellow River and Yangtze River, China, during the past 2000 years. *The Holocene*, *13*(6), 933–940. https://doi.org/10.1191/0959683603hl680rr

Gentry, A. H., & Lopez-Parodi, J. (1980). Deforestation and increased flooding of the upper amazon. *Science*, *210*(4476), 1354–1356. https://doi.org/10.1126/science.210.4476.1354

Giosan, L., Ponton, C., Usman, M., Blusztajn, J., Fuller, D. Q., Galy, V., et al. (2017). Massive erosion in monsoonal central India linked to late Holocene land cover degradation. *Earth Surface Dynamics*, *5*(4), 781–789. https://doi.org/10.5194/esurf-5-781-2017

Guilderson, T. P., Reimer, P. J., & Brown, T. A. (2005). The boon and bane of radiocarbon dating. *Science*, *307*(5708), 362–364. https://doi.org/10.1126/science.1104164

Guo, L., Su, N., Zhu, C., & He, Q. (2018). How have the river discharges and sediment loads changed in the Changjiang River basin downstream of the Three Gorges Dam? *Journal of Hydrology*, *560*, 259–274. https://doi.org/10.1016/j.jhydrol.2018.03.035

Han, M. L. (2013). Agricultural technology associated with the immigrants from northern China and shift of economic center to South China. *Journal of Chinese Historical Studies* (4), 117–138. (In Chinese).

Ho, P.-T. (1955). The introduction of American food plants into China. *American Anthropologist*, *57*(2), 191–201. https://doi.org/10.1525/aa.1955.57.2.02a00020

Hobo, N., Makaske, B., Wallinga, J., & Middelkoop, H. (2014). Reconstruction of eroded and deposited sediment volumes of the embanked River Waal, The Netherlands, for the period AD 1631–present. *Earth Surface Processes and Landforms*, *39*(10), 1301–1318. https://doi.org/10.1002/esp.3525

Hori, K., Saito, Y., Zhao, Q., Cheng, X., Wang, P., Sato, Y., & Li, C. (2001). Sedimentary facies and Holocene progradation rates of the Changjiang (Yangtze) delta, China. *Geomorphology*, *41*(2–3), 233–248. https://doi.org/10.1016/S0169-555X(01)00119-2

Huntley, D. J., Godfrey-Smith, D. I., & Thewalt, M. L. W. (1985). Optical dating of sediments. *Nature*, *313*(5998), 105–107. https://doi.org/10.1038/313105a0

Ibáñez, C., Alcaraz, C., Caiola, N., Prado, P., Trobajo, R., Benito, X., et al. (2019). Basin-scale land use impacts on world deltas: Human vs natural forcings. *Global and Planetary Change*, *173*, 24–32. https://doi.org/10.1016/j.gloplacha.2018.12.003

Li, B., Li, C., & Shen, H. (2003). A preliminary study on sediment flux in the Changjiang Delta during the postglacial period. *Science in China—*, *46*(7), 743–752. https://doi.org/10.1360/03yd9065

Li, C., Chen, Q., Zhang, J., Yang, S., & Fan, D. (2000). Stratigraphy and paleoenvironmental changes in the Yangtze delta during the late quaternary. *Journal of Asian Earth Sciences*, *18*(4), 453–469. https://doi.org/10.1016/S1367-9120(99)00078-4

Li, M., Chen, Z., Yin, D., Chen, J., Wang, Z., & Sun, Q. (2011). Morphodynamic characteristics of the dextral diversion of the Yangtze River mouth, China: Tidal and the Coriolis Force controls. *Earth Surface Processes and Landforms*, *36*(5), 641–650. https://doi.org/10.1002/esp.2082

Liu, J., Saito, Y., Kong, X., Wang, H., Xiang, L., Wen, C., & Nakashima, R. (2010). Sedimentary record of environmental evolution off the Yangtze River estuary, East China Sea, during the last ~13,000 years, with special reference to the influence of the Yellow River on the Yangtze River delta during the last 600 years. *Quaternary Science Reviews*, *29*(17–18), 2424–2438. https://doi.org/10.1016/j.quascirev.2010.06.016

Lu, X. (2016). *The man-land relationship and regional society in the middle reach of Yangtze River*. Xiamen University Press. (In Chinese).

Maselli, V., & Trincardi, F. (2013). Man made deltas. *Scientific Reports*, *3*(1), 1926. https://doi.org/10.1038/srep01926

Middelkoop, H., Erkens, G., & van der Perk, M. (2010). The Rhine delta—A record of sediment trapping over time scales from millennia to decades. *Journal of Soils and Sediments*, *10*(4), 628–639. https://doi.org/10.1007/s11368-010-0237-z

Murray, A., Arnold, L. J., Buylaert, J.-P., Guérin, G., Qin, J., Singhvi, A. K., et al. (2021). Optically stimulated luminescence dating using quartz. *Nature Reviews Methods Primers*, *1*(1), 72. https://doi.org/10.1038/s43586-021-00068-5

Nageswara Rao, K., Saito, Y., Nagakumar, K. C. V., Demudu, G., Rajawat, A. S., Kubo, S., & Li, Z. (2015). Palaeogeography and evolution of the Godavari delta, East Coast of India during the Holocene: An example of wave-dominated and fan-delta settings. *Palaeogeography, Palaeoclimatology, Palaeoecology*, *440*, 213–233. https://doi.org/10.1016/j.palaeo.2015.09.006

National Bureau of Statistics of China. (1953–2010). (In Chinese). Retrieved from http://www.stats.gov.cn/

Nian, X. M., & Zhang, W. G. (2018). Application of optically stimulated luminescence dating to Late Quaternary coastal deposits in China. (In Chinese). *Quaternary Sciences*, *38*(3), 573–586. https://doi.org/10.11928/j.issn.1001-7410.2018.03.03

Nian, X. M., Zhang, W. G., Wang, Z. H., Sun, Q. L., & Chen, Z. Y. (2021). Inter-comparison of optically stimulated luminescence (OSL) ages between different fractions of Holocene deposits from the Yangtze delta and its environmental implications. *Marine Geology*, *432*, 106401. https://doi.org/10.1016/j.margeo.2020.106401

Qin, J., Shi, A., Ren, G., Chen, Z., Yang, Y., Zou, X., & Zhang, P. (2020). Severe historical droughts carved on rock in the Yangtze. *Bulletin of the American Meteorological Society*, *101*(6), 905–916. https://doi.org/10.1175/BAMS-D-19-0126.1

Shang, Y., Nian, X., Zhang, W., & Wang, F. (2021). Yellow River's contribution to the building of Yangtze delta during the last 500 Years—Evidence from detrital zircon U-Pb geochronology. *Geophysical Research Letters*, *48*(14), e2020GL091896. https://doi.org/10.1029/2020GL091896

Shen, H., Li, J., Zhu, H., & Zhou, F. (1983). Transport of suspended sediments in the Changjiang estuary. *Proceedings of the International symposium on sedimentation on the continental shelf, with special reference to the East China Sea*, (In Chinese), (Vol. l, pp. 389–399). China Ocean Press.

Shen, Z., Törnqvist, T. E., Mauz, B., Chamberlain, E. L., Nijhuis, A. G., & Sandoval, L. (2015). Episodic overbank deposition as a dominant mechanism of floodplain and delta-plain aggradation. *Geology*, *43*(10), 875–878. https://doi.org/10.1130/g36847.1

Stanley, D. J., & Chen, Z. (2000). Radiocarbon Dates in China's Holocene Yangtze Delta: Record of sediment storage and reworking, not timing of deposition. *Journal of Coastal Research*, *16*(4), 1126–1132.

Stanley, D. J., & Warne, A. G. (1994). Worldwide initiation of Holocene marine deltas by deceleration of sea-level rise. *Science*, *265*(5169), 228–231. https://doi.org/10.1126/science.265.5169.228

Storozum, M. J., Zhen, Q., Xiaolin, R., Haiming, L., Yifu, C., Kui, F., & Haiwang, L. (2018). The collapse of the north Song dynasty and the AD 1048–1128 Yellow River floods: Geoarchaeological evidence from northern Henan province, China. *The Holocene*, *28*(11), 1759–1770. https://doi.org/10.1177/0959683618788682

Syvitski, J. P. M., Kettner, A. J., Overeem, I., Hutton, E. W. H., Hannon, M. T., Brakenridge, G. R., et al. (2009). Sinking deltas due to human activities. *Nature Geoscience*, *2*(10), 681–686. https://doi.org/10.1038/ngeo629

Tamura, T., Nguyen, V. L., Ta, T. K. O., Bateman, M. D., Gugliotta, M., Anthony, E. J., et al. (2020). Long-term sediment decline causes ongoing shrinkage of the Mekong megadelta, Vietnam. *Scientific Reports*, *10*(1), 8085. https://doi.org/10.1038/s41598-020-64630-z

Tamura, T., Saito, Y., Nguyen, V. L., Ta, T. K. O., Bateman, M. D., Matsumoto, D., & Yamashita, S. (2012). Origin and evolution of interdistributary delta plains; insights from Mekong River delta. *Geology*, *40*(4), 303–306. https://doi.org/10.1130/g32717.1

Tamura, T., Saito, Y., Sieng, S., Ben, B., Kong, M., Sim, I., et al. (2009). Initiation of the Mekong river Delta at 8 ka: Evidence from the sedimentary succession in the Cambodian lowland. *Quaternary Science Reviews*, *28*(3–4), 327–344. https://doi.org/10.1016/j.quascirev.2008.10.010

Tan, Q. (1982). *The historical atlas of China*. China Cartographic Publishing House. (In Chinese).

Wang, F., Zhang, W., Nian, X., Ge, C., Zhao, X., Cheng, Q., et al. (2019). Refining the late-Holocene coastline and delta development of the northern Yangtze River delta: Combining historical archives and OSL dating. *The Holocene*, *29*(9), 1439–1449. https://doi.org/10.1177/0959683619854522

Wang, F., Zhang, W., Nian, X., Roberts, A. P., Zhao, X., Shang, Y., et al. (2020). Magnetic evidence for Yellow River sediment in the late Holocene deposit of the Yangtze River delta, China. *Marine Geology*, *427*, 106274. https://doi.org/10.1016/j.margeo.2020.106274

Wang, Y., Cheng, H., Edwards, R. L., He, Y., Kong, X., An, Z., et al. (2005). The Holocene Asian monsoon: Links to solar changes and North Atlantic climate. *Science*, *308*(5723), 854–857. https://doi.org/10.1126/science.1106296

Wang, Z., Saito, Y., Zhan, Q., Nian, X., Pan, D., Wang, L., et al. (2018). Three-dimensional evolution of the Yangtze River mouth, China during the Holocene: Impacts of sea level, climate and human activity. *Earth-Science Reviews*, *185*, 938–955. https://doi.org/10.1016/j.earscirev.2018.08.012

Wohl, E., Bledsoe, B. P., Jacobson, R. B., Poff, N. L., Rathburn, S. L., Walters, D. M., & Wilcox, A. C. (2015). The natural sediment regime in rivers: Broadening the foundation for ecosystem management. *BioScience*, *65*(4), 358–371. https://doi.org/10.1093/biosci/biv002

Woodbridge, J., Fyfe, R. M., Roberts, N., Downey, S., Edinborough, K., & Shennan, S. (2014). The impact of the Neolithic agricultural transition in Britain: A comparison of pollen-based land-cover and archaeological ^{14}C date-inferred population change. *Journal of Archaeological Science*, *51*, 216–224. https://doi.org/10.1016/j.jas.2012.10.025

Yang, S. L., Milliman, J. D., Xu, K. H., Deng, B., Zhang, X. Y., & Luo, X. X. (2014). Downstream sedimentary and geomorphic impacts of the three gorges dam on the Yangtze River. *Earth-Science Reviews*, *138*, 469–486. https://doi.org/10.1016/j.earscirev.2014.07.006

Yang, S. L., Xu, K. H., Milliman, J. D., Yang, H. F., & Wu, C. S. (2015). Decline of Yangtze River water and sediment discharge: Impact from natural and anthropogenic changes. *Scientific Reports*, *5*(1), 12581. https://doi.org/10.1038/srep12581

Yin, H., & Li, C. (2001). Human impact on floods and flood disasters on the Yangtze River. *Geomorphology*, *41*(2), 105–109. https://doi.org/10.1016/S0169-555X(01)00108-8

Zhang, D. X. (2000). The effect of population activity on the changes in vegetation of Yangtze River Valley since the ancient period of Spring and Autumn-Warring States (770~221 B.C.). (In Chinese). *Journal of Plant Resources and Environment*, *9*, 47–53.

Zhang, H., Ait Brahim, Y., Li, H., Zhao, J., Kathayat, G., Tian, Y., et al. (2019). The Asian summer monsoon: Teleconnections and forcing mechanisms—A review from Chinese speleothem δ^{18}O records. *Quaternary*, *2*(3), 1–38. https://doi.org/10.3390/quat2030026

Zhang, R. S. (1984). Land-forming history of the Huanghe River delta and coastal plain of northern Jiangsu. (In Chinese). *Acta Geographica Sinica*, *39*, 173–184.

Zhang, X., Tang, Q., Liu, X., Leng, G., & Di, C. (2018). Nonlinearity of runoff response to global mean temperature change over major global river basins. *Geophysical Research Letters*, *45*(12), 6109–6116. https://doi.org/10.1029/2018GL078646

Zhang, X. G. (1998). A discussion on the land formation of Pudong area in Shanghai. (In Chinese). *Acta Geographica Sinica*, *53*(3), 228–237.

Zheng, J., Hao, Z., Fang, X., & Ge, Q. (2014). Changing characteristics of extreme climate events during past 2000 years in China. (In Chinese). *Progress in Geography*, *33*, 3–12. https://doi.org/10.11820/dlkxjz.2014.01.001

Zhou, X., Zhao, P., Liu, G., & Zhou, T. (2011). Characteristics of decadal-centennial-scale changes in East Asian summer monsoon circulation and precipitation during the Medieval Warm Period and Little Ice Age and in the present day. *Chinese Science Bulletin*, *56*(28), 3003. https://doi.org/10.1007/s11434-011-4651-4

References From the Supporting Information

Arnold, L. J., Bailey, R. M., & Tucker, G. E. (2007). Statistical treatment of fluvial dose distributions from southern Colorado arroyo deposits. *Quaternary Geochronology*, *2*(1), 162–167. https://doi.org/10.1016/j.quageo.2006.05.003

Ballarini, M., Wallinga, J., Wintle, A. G., & Bos, A. J. J. (2007). A modified SAR protocol for optical dating of individual grains from young quartz samples. *Radiation Measurements*, *42*(3), 360–369. https://doi.org/10.1016/j.radmeas.2006.12.016

Chen, Y., Zhang, W., Nian, X., Sun, Q., Ge, C., Hutchinson, S. M., et al. (2021). Greigite as an indicator for salinity and sedimentation rate change: Evidence from the Yangtze River delta, China. *Journal of Geophysical Research: Solid Earth*, *126*(3), e2020JB021085. https://doi.org/10.1029/2020JB021085

Cheng, Q., Wang, F., Chen, J., Ge, C., Chen, Y., Zhao, X., et al. (2020). Combined chronological and mineral magnetic approaches to reveal age variations and stratigraphic heterogeneity in the Yangtze River subaqueous delta. *Geomorphology*, *359*, 107163. https://doi.org/10.1016/j.geomorph.2020.107163

Dong, Y. (2014). *Magnetic properties and their paleoenvironmental implications of sediments in Holocene from Nantong coastal region*, PhD thesis, East China Normal University, Shanghai. (In Chinese).

Duller, G. A. T. (2003). Distinguishing quartz and feldspar in single grain luminescence measurements. *Radiation Measurements*, *37*(2), 161–165. https://doi.org/10.1016/S1350-4487(02)00170-1

Durcan, J. A., King, G. E., & Duller, G. A. T. (2015). DRAC: Dose Rate and Age Calculator for trapped charge dating. *Quaternary Geochronology*, *28*, 54–61. https://doi.org/10.1016/j.quageo.2015.03.012

Galbraith, R. F., Roberts, R. G., Laslett, G. M., Yoshida, H., & Olley, J. M. (1999). Optical dating of single and multiple grains of quartz from Jinmium rock shelter, northern Australia: Part I, experimental design and statistical models. *Archaeometry*, *41*(2), 339–364. https://doi.org/10.1111/j.1475-4754.1999.tb00987.x

Gao, L., Long, H., Shen, J., Yu, G., Liao, M., & Yin, Y. (2017). Optical dating of Holocene tidal deposits from the southwestern coast of the South Yellow Sea using different grain-size quartz fractions. *Journal of Asian Earth Sciences*, *135*, 155–165. https://doi.org/10.1016/j.jseaes.2016.12.036

Gao, L., Long, H., Shen, J., Yu, G., & Yin, Y. (2016). High-resolution OSL dating of a coastal sediment sequence from the South Yellow Sea. *Geochronometria*, *43*(1), 143–154. https://doi.org/10.1515/geochr-2015-0044

Gao, L., Long, H., Zhang, P., Tamura, T., Feng, W., & Mei, Q. (2019). The sedimentary evolution of Yangtze River delta since MIS3: A new chronology evidence revealed by OSL dating. *Quaternary Geochronology*, *49*, 153–158. https://doi.org/10.1016/j.quageo.2018.03.010

Guérin, G., Mercier, N., & Adamiec, G. (2011). Dose-rate conversion factors: Update. *Ancient TL*, *29*, 5–8.

Heaton, T. J., Köhler, P., Butzin, M., Bard, E., Reimer, R. W., Austin, W. E. N., et al. (2020). Marine20—The marine radiocarbon age calibration curve (0–55,000 cal BP). *Radiocarbon*, *62*(4), 779–820. https://doi.org/10.1017/RDC.2020.68

Hori, K., & Saito, Y. (2017). Differences in radiocarbon ages among molluscan shells, plant materials, and total organic carbon: An example from the paleo-Changjiang incised-valley fill, China. *Quaternary International*, *455*, 45–55. https://doi.org/10.1016/j.quaint.2017.07.037

Hori, K., Saito, Y., Zhao, Q., Cheng, X., Wang, P., Sato, Y., & Li, C. (2001). Sedimentary facies of the tide-dominated paleo-Changjiang (Yangtze) estuary during the last transgression. *Marine Geology*, *177*(3–4), 331–351. https://doi.org/10.1016/S0025-3227(01)00165-7

Lu, Y. (2019). *Magnetic Characteristics and Indication Significance of Orifice A5-3 and A6-5 in Yangtze Estuary Submerged Delta*. MSc thesis, Shanghai Normal University. (In Chinese).

Murray, A. S., & Wintle, A. G. (2000). Luminescence dating of quartz using an improved single-aliquot regenerative-dose protocol. *Radiation Measurements*, *32*(1), 57–73. https://doi.org/10.1016/S1350-4487(99)00253-X

Nian, X., Zhang, W., Wang, Z., Sun, Q., Chen, J., & Chen, Z. (2018). Optical dating of Holocene sediments from the Yangtze River (Changjiang) Delta, China. *Quaternary International*, *467*, 251–263. https://doi.org/10.1016/j.quaint.2018.01.011

Nian, X., Zhang, W., Wang, Z., Sun, Q., Chen, J., Chen, Z., & Hutchinson, S. M. (2018). The chronology of a sediment core from incised valley of the Yangtze River delta: Comparative OSL and AMS ^{14}C dating. *Marine Geology*, *395*, 320–330. https://doi.org/10.1016/j.margeo.2017.11.008

Pan, D., Chen, T., Zhan, Q., & Wang, Z. (2017). Mineral magnetic properties of Holocene sediments in the subaqueous Yangtze delta and the implications for human activity and early diagenesis. *Quaternary International*, *459*, 133–143. https://doi.org/10.1016/j.quaint.2017.05.010

Reimer, P. J., Austin, W. E. N., Bard, E., Bayliss, A., Blackwell, P. G., Bronk Ramsey, C., et al. (2020). The IntCal20 northern hemisphere radiocarbon age calibration curve (0–55 cal kBP). *Radiocarbon*, *62*(4), 725–757. https://doi.org/10.1017/RDC.2020.41

Stuiver, M., Reimer, P. J., & Reimer, R. W. (2021). CALIB 8.2. Retrieved from http://calib.org

Su, J., Fan, D., Leng, W., Chen, L., & Yin, P. (2017). Postglacial sequence stratigraphy and sedimentary environment evolution of the Yangtze River subaqueous delta. *Journal of Palaeogeography*, *19*(3), 541–556. (In Chinese). https://doi.org/10.7605/gdlxb.2017.03.042

Sugisaki, S., Buylaert, J.-P., Murray, A., Tada, R., Zheng, H., Ke, W., et al. (2015). OSL dating of fine-grained quartz from Holocene Yangtze delta sediments. *Quaternary Geochronology*, *30*, 226–232. https://doi.org/10.1016/j.quageo.2015.02.021

Wang, F., Nian, X., Wang, J., Zhang, W., Peng, G., Ge, C., et al. (2018). Multiple dating approaches applied to the recent sediments in the Yangtze River (Changjiang) subaqueous delta. *The Holocene*, *28*(6), 858–866. https://doi.org/10.1177/0959683617752847

Wang, M., Zheng, H., Xie, X., Fan, D., Yang, S., Zhao, Q., & Wang, K. (2011). A 600-year flood history in the Yangtze River drainage: Comparison between a subaqueous delta and historical records. *Chinese Science Bulletin*, *56*(2), 188–195. https://doi.org/10.1007/s11434-010-4212-2

Wang, Y., Zhang, Y., Zou, X., Zhu, D., & Piper, D. (2012). The sand ridge field of the South Yellow Sea: Origin by river–sea interaction. *Marine Geology*, *291–294*, 132–146. https://doi.org/10.1016/j.margeo.2011.01.001

Wang, Z., Li, M., Zhang, R., Zhuang, C., Liu, Y., Saito, Y., et al. (2011). Impacts of human activity on the late-Holocene development of the subaqueous Yangtze delta, China, as shown by magnetic properties and sediment accumulation rates. *The Holocene*, *21*(3), 393–407. https://doi.org/10.1177/0959683610378885

Wang, Z., Xu, H., Zhan, Q., Saito, Y., He, Z., Xie, J., et al. (2010). Lithological and palynological evidence of late Quaternary depositional environments in the subaqueous Yangtze delta, China. *Quaternary Research*, *73*(3), 550–562. https://doi.org/10.1016/j.yqres.2009.11.001

Xu, T., Shi, X., Wang, G., Qiao, S., Yang, G., Liu, S., et al. (2013). Sedimentary facies of the subaqueous Changjiang River delta since the late Pleistocene. *Chinese Journal of Oceanology and Limnology*, *31*(5), 1107–1119. https://doi.org/10.1007/s00343-013-2281-1

Xu, T., Wang, G., Shi, X., Wang, X., Yao, Z., Yang, G., et al. (2016). Sequence stratigraphy of the subaqueous Changjiang (Yangtze River) delta since the Last Glacial Maximum. *Sedimentary Geology*, *331*, 132–147. https://doi.org/10.1016/j.sedgeo.2015.10.014

Yi, S., Saito, Y., Chen, Z., & Yang, D. Y. (2006). Palynological study on vegetation and climatic change in the subaqueous Changjiang (Yangtze River) delta, China, during the past about 1600 years. *Geosciences Journal*, *10*(1), 17–22. https://doi.org/10.1007/BF02910329

Zhou, K., Meng, Y., & Zhang, J. (2012). Sediment characteristics of core DT from the east end of Chongming Dongtan, Changjiang River estuary and its environmental implication. *Quaternary Sciences*, *32*(6), 1173–1182. (In Chinese). https://doi.org/10.3969/j.issn.1001-7410.2012.06.11